Atmospheric Metal Doping System and Application for Poly-Si Backplane

D. H. SHIN, J. M. LEE, S. K. LEE, and H, J, KIM
Research Center of VIATRON TECHNOLOGIES Inc., Gasan-dong, Gumcheon-gu, Seoul 153-803, Korea
TEL:82-2-839-4100, e-mail: shindh@viatrontech.com

Keywords : MIC poly-Si, metal doping, crystallization

Abstract

VIATRON TECHNOLOGIES has developed an Atmospheric Metal Doping (AMD) system which uniformly dopes metal species onto a substrate. The AMD system injects metal-organic vapor over substrate using an injection head with a scan motion. One of important application of this system is a metal-induced crystallization of amorphous Si for manufacturing AMOLED poly-Si panels. The AMD system with a use of Ni vapor source produces doping of trace amount of Ni onto amorphous Si, enabling uniform MIC crystallization. Also, the operation without vacuum condition offers advantages such as easy maintenance, low cost production, and large glass processes.

1. Introduction

Recently, Metal Induced Crystallization (MIC) process of amorphous Si is considered to be one of promising way to produce poly-Si for AMOLED displays. Several major AMOLED companies are developing their own advanced MIC processes such as Continuous Grain Silicon (CGS), Super Grain Silicon (SGS), Nano-cap Assisted Crystallization (NAC)[1-3].

For the MIC processes to be accepted as an industrial production method, leakage current problem of poly-Si TFTs associated with metal contamination should be solved. One approach is to minimize the amount of metal addition. Recently, it has been reported that amount of added Ni, most common metal for MIC, can be minimized by capping layers[4]. This process can produce poly-Si with large grain structure through selective area crystallization and subsequent large lateral growth. Even though this method gives the high quality poly-Si, it requires additional process steps. In this regard, the process which produces large poly-Si grains without capping layers will be beneficial for cost-effective production of MIC-based poly-Si.

Viatron Technologies Inc. has developed the Ni doping system, referred to *Atmospheric Metal Doping (AMD)* system. This system incorporates injection of Ni vapor onto a-Si glass using an injector unit. The injector head is moving with scan direction to give uniform doping over large glass substrate. In this paper, we will discuss about the performance of AMD system, and its' application to MIC processes.

2. AMD system

Fig. 1 shows the picture of AMD system. The AMD system consists of vaporization units of liquid Ni source, vapor injector, and glass heating susceptor. The vapor injector moves over glass surface with a linear robot.

Fig. 1. Atmospheric Metal Doping system

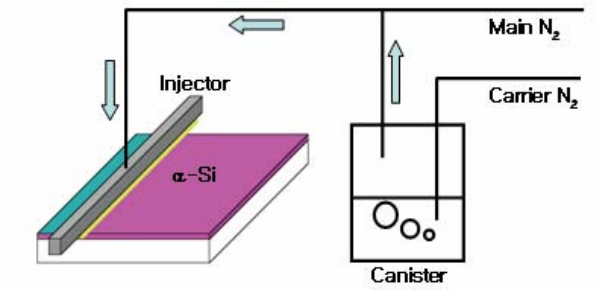

Fig. 2. Schematic diagram of AMD system.

The Fig.2 is the schematic description of operation of AMD system. The Ni vapor is injected onto a-Si glass surface. The AMD system uses the Viatron's patented liquid Ni source. The Ni source has high vapor pressure (0.23 Torr at 70°C) and provides Ni vapor sufficient for processing large glass at short time. The Ni vapor is chemically stable without thermal decomposition. The residue after complete vaporization of Ni source is less than 0.5%, indicating congruent vaporization chemically.

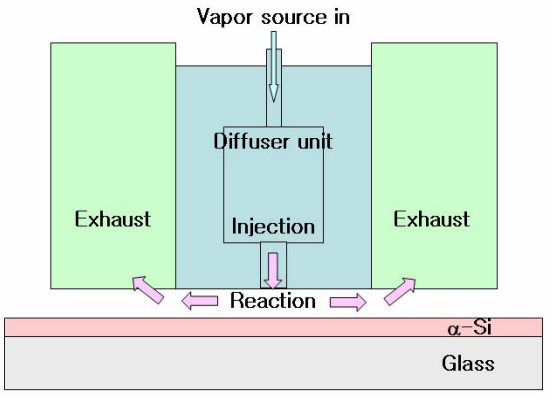

Fig. 3. Diagram of injector unit

The schematic description of injection unit is shown in Fig. 3 The injector unit consists of multiple diffuser layers to achieve a uniform vapor flow along length direction. The variation of flow velocity is less than 5% over length positions, as shown in Fig. 4 The injected Ni vapor reacts with a-Si films on the glasses which is heated at 150~250°C. The by-product gases flow into exhaust unit in the injector body, so that gas flow is confined within injection area. Before the process begins, whole injection unit is purged with N_2 gas to make an inert ambient.

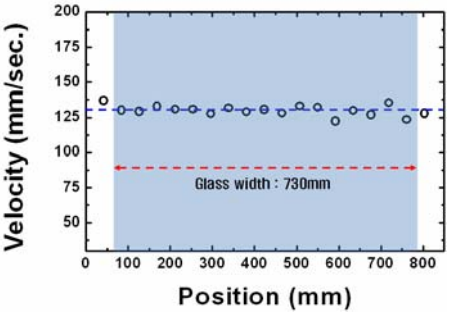

Fig. 4. Variation of flow velocity plotted against position.

3. Processes

3.1 Ni doping and crystallization

The amount of Ni doping and uniformity can be evaluated by measuring grain size distributions of the poly-Si after crystallization. The typical crystallization behavior in MIC is shown in Fig. 5.

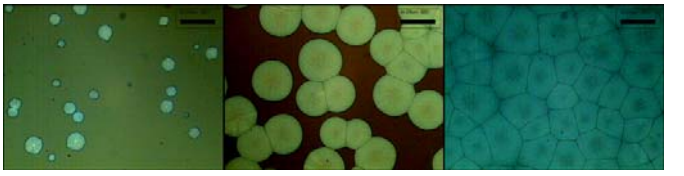

Fig. 5. Optical micrographs showing evolution of large poly-Si grains during MIC crystallization.

The Ni vapor reacts with a-Si to form Ni silicides which serve as nucleation seeds for subsequent lateral growth. The seeds grow laterally until they impinge each other to form large grains. It is interesting to note that this crystallization mechanism has been only reported in the Ni deposition with capping layers, e.g., SGS, NAC, MICC[2-4]. This result, however, indicates that the large grains can be achieved without capping layer utilizing the AMD method. The MIC poly-Si with large grains has been reported to have superior TFT characteristics.

One of advantages of AMD system is an easy control the Ni concentration. The Ni concentration can be controlled by changing Ni vaporization temperature, glass temperature, and injection scan speed. Fig. 6 shows the grain size after MIC crystallization plotted against scan speeds for the cases with and without capping layers. Optical micrographs showing grain structure are also shown in Fig. 7. The grain sizes increase with increasing scan speed. This result can be explained by less amount of

Ni doping at higher scan speed.

As can be seen in Fig. 6, increase of grain size does not show linear dependency on the scan speed. The dependency can be categorized into three regimes as marked in the figure. Regime I shows strong dependency on scan speed. Also, in this regime, the poly-Si has uniform distribution of small grains (Fig. 7a).

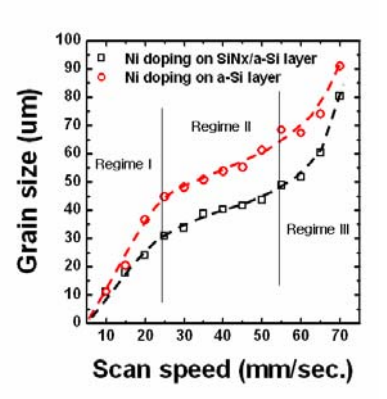

Fig. 6. Grain sizes plotted against scan speed

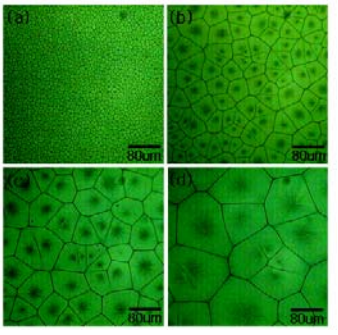

Fig. 7 Grain structures at scan speeds of (a) 15 mm/sec, (b) 30 mm/sec, (c) 50 mm/sec, and (d) 70 mm/sec.

In Regime II, the dependency is weaker than those of Regime I and III. The grain structure in this regime is characterized by mixture of large and small grains, as shown in Fig. 7b and 7c. Regime III shows the strong dependency and uniform size distribution (Fig. 7d), similar to regime I. This non-linear dependency may be associated with changes of nucleation and growth kinetics and re-distribution of Ni during the course of crystallization,

3.2 Doping uniformity

AMD system has very good doping uniformity. We evaluate the uniformity by measuring the grain size in the 150 sample pieces with 5mmX5mm taken from 730X920 mm area. Fig. 8 is the grain size distribution when we set the condition to obtain the grain size of 15 ㎛. The average grain size is 15.1 ㎛ and its standard deviation is 1.55 ㎛ with an effective area of 97.5% of Gen 4 glass.

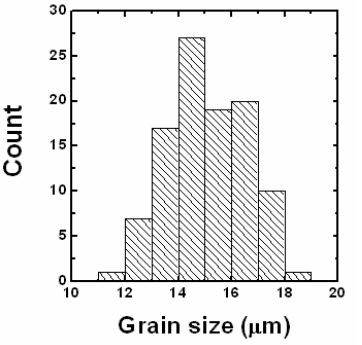

Fig. 8. Histogram of grain size distributions.

3.3 Quality of poly-Si

The crystallization heat treatment is carried out using Viatron's Field Enhanced Rapid Thermal Processor (FE-RTP) system. The detail explanation of FE-RTP system has been reported in the previous paper [5]. The system is able to heat the glasses to high temperatures up to 800°C without thermal glass damages. Also, the rapid heating capability with field induction enables fast crystallization and high production rate.

We investigate the crystallinity of poly-Si using UV-visible transmittance. We reported that the UV slope value taken from UV-visible transmittance spectra proportionally represents the crystalline-to-amorphous Si ratio in the Si films. The computer simulation using optical parameters of amorphous and crystalline Si suggests that single crystal Si films have the UV slope value of 1.8 and a-Si has ~0.2 around 450 nm for 500Å-thick Si films[6].

Fig. 9 shows a UV slope value versus crystallization temperature. The total heat treatment time was fixed at 15 mins. UV slope value linearly increases with annealing temperature from 650℃ to 750℃. The results indicate that significant residual a-Si still remains after low temperature crystallization. The residual a-Si is not removed completely even after long crystallization time (several hours) at the low temperature ranges below 650℃. Since the presence of residual a-Si is known to cause high leakage currents of the poly-Si TFTs[7], high temperature crystallization is important for high performance TFTs. The high temperature process is

also beneficial to improve the crystallinity of poly-Si by annealing out some intra-granular defects.

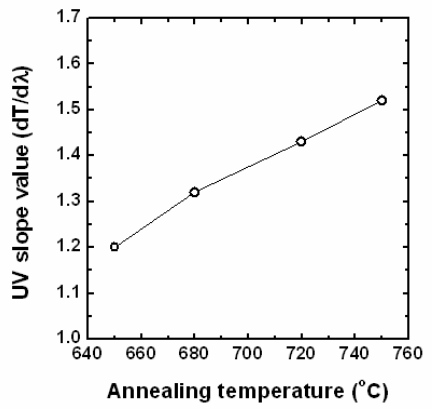

Fig. 9. UV slope values at various crystallization temperatures.

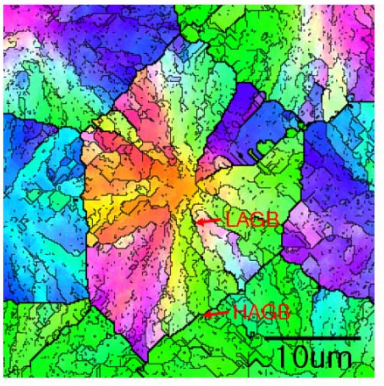

Fig. 10. Typical EBSD image of MIC poly-Si.

To investigate the detail grain structure of MIC poly-Si, Electron Back Scattered Diffraction (EBSD) is carried out. Fig. 8 is a typical EBSD image of MIC poly-Si. The image clearly shows the crystallization evolutions of MIC. Ni silicides at the center of grains act as nucleation sites, and the seeds propagate in the radial direction to form the large grains. From this mechanism, it is believed that the grain boundaries contain substantial Ni concentration (or is composed of Ni silicides). EBSD pole mapping indicates that many of seeds grow with different crystallographic orientations inside grains, leading to formation of sub-grains which have both high and low angle grain boundaries. The additional high temperature annealing after crystallization will be an effective method to remove the sub-grain boundaries, hence, improving the poly-Si qualities.

4. Conclusion

Viatron Technologies has developed Atmospheric Metal Doping system which enables the doping of trace amount of metal species over large substrate. The AMD system utilizes the injection of metal vapor using moving injector onto substrate. AMD system with Ni vapor source is able to produce uniform poly-Si panels through advanced metal-induced crystallization. The non-vacuum process of AMD system gives advantages such as easy maintenance, low cost process, and large glass treatments.

5. Acknowledgements

The authors would like to thank to professor K. W. Oh for providing EBSD analysis.

6. References

1. T. Mizuki et al., IEEE Trans. Electron Devices, **51**, p.204(2004)
2. H. K. Chung, K. Y. Lee, SID 05 DIGEST, 956-959
3. Y. J. Chang, Y. I. Kim, S. H. Shim, S. Park, K. W. Ahn, S. C. Song, J. B. Choi, H. K. Min, C. W. Kim, SID 06 DIGEST, 1276-1279
4. J. H. Oh, S. H. Kim, J. W. Choi, D. H. Kang, E. Y. Lee, J. H. Hur, J. Jang, SID 06 DIGEST, 262-265
5. H. J. Kim, D. H. Shin, IMID/IDMC '06 DIGEST, 533-536
6. S. H. Lee, D. H. Shin, H. J. Kim, S. H. Park, and J. S. Lee, J. Ther. Sci. **46**, p.399-406(2007)
7. M. Wang, Z. Meng, Y. Zohar, M. Wong, IEEE Trans. Electron Devices, **48**, p.794-800 (2001)